The Journal of Infectious Diseases

MAJOR ARTICLE

Ampicillin/Sulbactam in Combination with Ceftazidime/Avibactam Against Metallo-β-Lactamase-Producing Carbapenem-Resistant *Acinetobacter baumannii*: A Genomics-Informed Mechanism-based model

Bhavatharini Arun,[1,a] Eloise Liu,[1,a] Quentin Vallé,[1] Rajnikant Sharma,[1] Ngoc Minh Bui,[1] Vyanka Mezcord,[2] Irene Luu,[2] German Matias Traglia,[3] Fernando Pasteran,[4] David Paterson,[5] Robert A. Bonomo,[6] María Soledad Ramirez,[2] and Gauri G. Rao[1]

[1]Department of Clinical Pharmacy, USC Alfred E. Mann School of Pharmacy and Pharmaceutical Sciences, University of Southern California, Los Angeles, California, USA; [2]Center for Applied Biotechnology Studies, Department of Biological Science, College of Natural Sciences and Mathematics, California State University Fullerton, Fullerton, California, USA; [3]Unidad de Genomica y Bioinformatica, Departamento de Ciencias Biológicas, CENUR Litoral Norte, Universidad de la República, Salto, Uruguay; [4]National Regional Reference Laboratory for Antimicrobial Resistance (NRL), Servicio Antimicrobianos, Instituto Nacional de Enfermedades Infecciosas, ANLIS Dr. Carlos G. Malbrán, Buenos Aires, Argentina; [5]Saw Swee Hock School of Public Health, National University of Singapore, Singapore, Singapore; and [6]Division of Infectious Diseases, Department of Medicine, Case Western Reserve University School of Medicine, Cleveland, Ohio, USA

Background. Carbapenem-resistant *Acinetobacter baumannii* (CRAB) infections, driven by metallo- and class-D serine β-lactamases, pose significant therapeutic challenges. β-Lactam-based combinations offer a promising alternative to agents like colistin and tigecycline, which are associated with toxicity, and to cefiderocol, which is facing emerging resistance.

Methods. The pharmacodynamic activity of ampicillin/sulbactam and ceftazidime/avibactam was evaluated against three CRAB strains: AMA3, AMA133, and AMA205. Genotypic and phenotypic resistance profiles were characterized, and antibacterial activity was assessed using static concentration time-kill (SCTK) assays. A mechanism-based pharmacodynamic model (MBM) was developed using SCTK data, incorporating the bacterial resistome. This model informed the design of in vitro dynamic infection model studies, which were subsequently used to validate MBM predictions.

Results. These strains harboring resistance genes including $bla_{\text{OXA-23}}$ (AMA133), $bla_{\text{NDM-1}}$ (AMA3), or both (AMA205) were resistant to ampicillin/sulbactam and ceftazidime/avibactam. However, combination therapy significantly reduced bacterial burden, achieving approximately 90% reduction in the area under the $\log_{10}$-CFU-versus-time curve for AMA133, and approximately 50–70% for AMA3 and AMA205.

The MBM incorporated sulbactam hydrolysis by NDM-1 and OXA23 enzymes, along with drug acylation kinetics to penicillin-binding proteins. Potency (*EC*50) estimates revealed a resistance hierarchy: AMA3 > AMA205 > AMA133. Avibactam notably enhanced sulbactam's activity. Simulations and experimental validation demonstrated that high-dose ampicillin/sulbactam combinations were required to achieve 4–6 $\log_{10}$-CFU reductions in $bla_{\text{NDM-1}}$ strains, while lower doses sufficed for AMA133.

Conclusions. This study highlights the potential of integrating genomic insights into MBM to optimize antibiotic regimens. The ampicillin/sulbactam and ceftazidime/avibactam combinations demonstrated promising activity against highly resistant CRAB strains, supporting their potential for clinical application in managing difficult-to-treat infections.

Keywords. carbapenem-resistant *Acinetobacter baumannii*; metallo-β-lactamases; antimicrobial resistance; mechanism-based modeling; pharmacokinetics/pharmacodynamics.

Carbapenem-resistant *Acinetobacter baumannii* (CRAB) is a significant global health threat, particularly among critically ill patients, with bloodstream infection mortality rates reaching up to 70% [1]. The Centers for Disease Control and Prevention (CDC) has classified CRAB as an urgent threat due to the limited efficacy of current treatment options and the pressing need for new therapeutic approaches [2].

CRAB's resistance is driven by both intrinsic and acquired mechanisms. Intrinsic resistance includes low-permeability outer membrane porins such as OmpA, intrinsically expressed β-lactamases, and multidrug efflux pumps like AdeABC and AdeIJK, which contribute to resistance against key antibiotics, including aztreonam (ATM) [3]. Acquired resistance,

Received 04 September 2025; accepted 07 November 2025; published online 12 November 2025

[a]B. A. and E. L. contributed equally to the study.

Correspondence: Gauri G. Rao, PharmD, MS, Department of Clinical Pharmacy, USC Alfred E. Mann School of Pharmacy and Pharmaceutical Sciences, University of Southern California, 1985 Zonal Avenue, PSC 304B3, Los Angeles, CA 90089 (gaurirao@usc.edu).

The Journal of Infectious Diseases®

https://doi.org/10.1093/infdis/jiaf567

primarily due to OXA-type β-lactamases, further complicates treatment [4]. Multidrug-resistant (MDR) *Acinetobacter* species expressing carbapenemases are highly resistant to ceftazidime/avibactam (CAZ/AVI), with reported rates exceeding 73.6% [5, 6]. Moreover, *A. baumannii*'s intrinsic resistance to ATM renders combinations such as CAZ/AVI with ATM ineffective against metallo-β-lactamase (MBL) producing CRAB. This ineffectiveness is attributed to limited membrane permeability and active efflux mechanisms, including OmpA-associated pathways [7]. The Infectious Diseases Society of America (IDSA) has emphasized that aztreonam is intrinsically inactive against *A. baumannii* [8], and Dumbleton et al. demonstrated that CAZ/AVI plus ATM failed to achieve ≥2 $\log_{10}$ CFU/mL killing at 24 hours in CRAB isolates [9]. Although cefiderocol was initially considered a promising salvage therapy for CRAB, post-hoc analysis of the CREDIBLE-CR trial revealed increased mortality among CRAB-infected patients treated with cefiderocol, potentially due to heteroresistance [10, 11]. Additionally, in vitro studies have documented NDM-mediated resistance to cefiderocol in *A. baumannii,* along with high cross-resistance between CAZ/AVI and cefiderocol in some species [12, 13].

While polymyxin and tigecycline-based regimens are widely used, their toxicity, inconsistent efficacy, and poor tissue penetration have led to increased interest in sulbactam-based combinations. High-dose ampicillin/sulbactam (AMP/SUL), in combination with other agents, has shown favorable outcomes in reducing mortality among critically ill CRAB patients and is now recommended as backbone therapy [14]. SUL, an irreversible β-lactamase inhibitor, can saturate penicillin-binding proteins (PBPs) at high doses [15]. However, SUL is susceptible to degradation by β-lactamases produced by CRAB.

Combining SUL with a broad-spectrum β-lactamase inhibitor like durlobactam (DUR) enhances antimicrobial activity, but the SUL/DUR combination remains ineffective against MBLs [16]. Moreover, access to SUL/DUR may be limited in low- and middle-income countries (LMICs). As a more accessible alternative, AVI was evaluated, given emerging evidence suggesting it may exert effects beyond β-lactamase inhibition. Notably, the SUL/AVI combination has demonstrated significant reductions in SUL's minimum inhibitory concentrations (MICs), against MBL-producing CRAB, potentially through mechanisms involving disruption of bacterial cell wall synthesis, modulation of efflux pump activity, and alterations in membrane permeability [17].

The objective of this study was to evaluate the efficacy of AMP/SUL and CAZ/AVI against clinical CRAB strains by integrating bacterial genomics, in vitro experiments, and in silico mathematical modeling. Next-generation sequencing (NGS) was employed to identify antimicrobial resistance (AMR) genes. Antibiotic efficacy at clinically relevant exposures was assessed using both static and dynamic in vitro infection models. A mechanism-based pharmacokinetic–pharmacodynamic (PK/PD) model (MBM) was developed, accounting for drug degradation by β-lactamases and PBP affinities. This model was further used to optimize dosing strategies and inform the design of the in vitro dynamic infection model (IVDIM), enabling robust validation of the MBM prediction.

METHODS

Antibiotics, Medium, and Bacterial Isolates

Three clinically isolated MDR CRAB strains, AMA3 and AMA133 (sequence type ST25), and AMA205 (ST79) were used in this study. Cation-adjusted Mueller–Hinton broth (CAMHB: 25 μg/mL Ca^{2+}, 12.5 μg/mL Mg^{2+}) and Mueller–Hinton II agar (BD Biosciences, Franklin Lakes, NJ) were used for all in vitro models. The antibiotics SUL (Sigma-Aldrich, St. Louis, MO), AMP (Sigma-Aldrich, St. Louis, MO), CAZ (Sigma-Aldrich, St. Louis, MO), and AVI (MedChemExpress, Monmouth Junction, NJ) were freshly prepared in sterile phosphate-buffered saline and filter sterilized using a 0.22 μm Millex GP syringe filter (Corning Inc., Corning, NY).

Phenotypic and Genotypic Antibiotic Susceptibility Testing

MICs for the three CRAB strains were determined for multiple agents, including AMP/SUL (256/128–0.5/0.25 μg/mL) and CAZ/AVI (256–0.5 μg/mL with fixed AVI concentration of 4 mg/L), using the broth microdilution method in triplicates, following Clinical and Laboratory Standards Institute guidelines [18]. To evaluate synergy, AMP/SUL (512/256–1/0.5 μg/mL) was tested in combination with fixed concentrations of CAZ/AVI (64/16, 32/8, and 16/4 μg/mL) or AVI (16, 8, and 4 μg/mL) in duplicates, assessing the fold reduction in MICs. The details of the whole-genome sequencing (WGS) and bioinformatic analysis are provided in the Supplementary Text.

Static Concentration Time-kill Assays

Static concentration time-kill (SCTK) assays were conducted using three CRAB isolates grown overnight in CAMHB. All experiments were performed with an initial inoculum of ~ 10^6 CFU/mL. Antibiotic concentrations were selected based on previously published human PK data for a dose of 2.5 g of CAZ/AVI [19, 20] (maximum plasma concentration C_{max} = 45–90.4 and 12.0–15.5 μg/mL for CAZ and AVI, respectively) and 2/1 g—8/4 g of AMP/SUL [21, 22], (C_{max} = 40.8–132 and 25.3–70.2 μg/mL for AMP and SUL, respectively) assuming 95% plasma protein binding for CAZ/AVI and 28% and 38% for AMP and SUL, respectively.

The experiments were conducted over 24 hours with AMP/SUL (2:1 ratio) at concentrations of 200/100, 100/50, and 25/12.5 μg/mL, and CAZ/AVI (4:1 ratio) at concentrations

Table 1. Antibiotic Regimens Simulated in the One-Compartment in Vitro Dynamic Infection Model (IVDIM)

Antibiotic Regimen	Simulated PK			Strain(s)	Clinical Evidence
	C_{max}* (μg/mL)	$T_{1/2}$ (h)	CL[a] (mL/h)		
AMP/SUL 8 g/4g as 2-h infusion every 8h	184/98.4	3	60	AMA205, AMA3	FDA-label[b] IDSA[c] recommendation Prospective[d] randomized trial
AMP/SUL 4 g/2g as 2-h infusion every 8h	89.3/47.6	3	60	AMA133	
CAZ/AVI 2 g/0.5g as 2-h infusion every 8h	57.6/11.0	3	60	AMA133, AMA205, AMA3	
AMP/SUL 8 g/4g+	184/98.4	3	60	AMA205, AMA3	
CAZ/AVI 2 g/0.5g as 2-h infusion every 8h	57.6/11.0	3	60		
AMP/SUL 4 g/2g+	89.3/47.6	3	60	AMA133, AMA205, AMA3	
CAZ/AVI 2 g/0.5g as 2-h infusion every 8h	57.6/11.0	3	60		
AMP/SUL 2 g/1g+	49.4/26.1	3	60	AMA133	
CAZ/AVI 2 g/0.5g as 2-h infusion every 8h	57.6/11.0	3	60		

Parameters from published population pharmacokinetic models for these antibiotics [27, 28] were used to simulate fC_{max}, accounting for protein binding: 28% for AMP, 38% for SUL, and 95% for both CAZ and avibactam AVI.

Abbreviations: AMP, ampicillin; SUL, sulbactam; CAZ, ceftazidime; AVI, avibactam; fC_{max}, unbound maximal plasma concentration; CL, clearance; $T_{1/2}$, elimination half-life.

[a]In vitro CL was simulated using the Masterflex peristaltic pump to reflect the $T_{1/2}$ of each drug. (CL = volume of the one-compartment IVDIM system × 0.693/$T_{1/2}$).

[b]Food and Drug Administration (FDA) recommendation: ≤ 4 g/day [25].

[c]Infectious Diseases Society of America (IDSA) recommendation: up to 9 g/day [26].

[d]Randomized trial in critically ill patients with ventilator-associated pneumonia by MDR *A. baumannii:* 24 g/12 g per day [27].

of 200/50, 100/25, and 25/6.25 μg/mL, as previously described [23]. Details of SCTK assay are included in the Supplementary Text.

One-Compartment in Vitro Dynamic Infection Model

A one-compartment IVDIM was used, as previously described [23], with an initial inoculum of ~ 10^7 CFU/mL over 72 hours, to evaluate the efficacy of AMP/SUL and CAZ/AVI as mono and combination therapies. The published half-lives of SUL and CAZ/AVI are 2.15 ± 1.16 hours and 2.6 ± 0.3 hours, respectively [19, 24]. Half-life of 3 hours was simulated for both drugs and the PK profiles for AMP/SUL and CAZ/AVI were simulated based on published population pharmacokinetic (PopPK) studies [19, 20]. Drug regimens were selected using MBM-based simulations of pharmacodynamic effects, informed by existing dosage regimens (Table 1) [25–27]. Details of the IVDIM experiment are included in the Supplementary Text.

Mechanism-based Model (MBM) Development and Simulations

The MBM was developed to characterize the pharmacodynamic effects of AMP/SUL and CAZ/AVI on bacterial growth and killing. This model incorporated natural growth dynamics of the bacteria and bacterial subpopulations with varying susceptibilities to SUL and CAZ. Drug effects were driven by bacterial enzyme–mediated hydrolysis and drug target interactions. Mechanistic synergy between the drugs along with subpopulation synergy, was integrated to gain mechanistic insights into the effects of combination therapy. Enzyme-mediated hydrolysis of SUL by NDM-1 and/or OXA-23 was described using Michaelis–Menten kinetics, with catalytic efficiency (K_{cat}) and substrate affinity (K_m) values specific to each enzyme, obtained from literature [29]. The drug effects were modeled using the Hill function and acylation rate constants of the respective drugs for purified PBP1a, PBP2, and PBP3 isolated from *A. baumannii* informed the *Emax* [28]. The final MBM model parameters were used to perform in silico simulations that guided drug-regimen selection for the IVDIM. Model development was conducted using the S-ADAPT software (version 1.57) with SADAPT-TRAN (pmethod = 4) [30]. Detailed model methods and codes are included in the Supplementary Text.

RESULTS

Phenotypic and Genotypic Antibiotic Susceptibility Testing

Figure 1 illustrates the resistome of the isolates with multiple genes from the same family grouped together for clarity, along with the phenotypic resistance (MIC changes). Genomic analysis identified both shared and strain-specific resistance mechanisms among the three CRAB isolates. Consistent with previous studies [31, 32], AMA3 and AMA205 harbored the MBL gene $bla_{\text{NDM-1}}$, while AMA133 carried $bla_{\text{OXA-23}}$, an acquired class-D β-lactamase associated with carbapenem resistance [3]. All three strains possessed intrinsic $bla_{\text{OXA-51-like}}$ genes and chromosomal ADC-type cephalosporinase genes

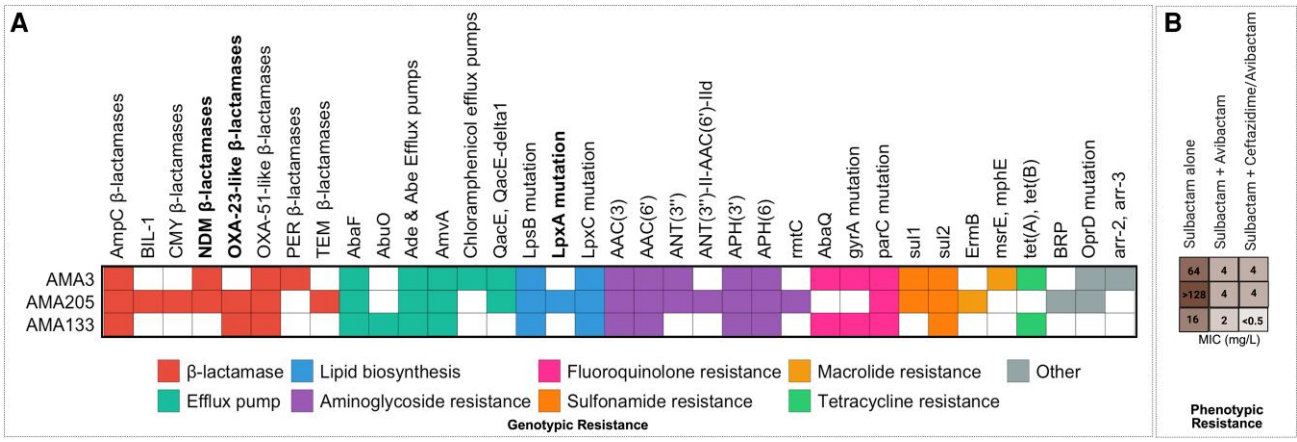

Figure 1. *A*, The genotypic resistance shows the antibiotic resistome for the three CRAB strains, AMA3, AMA205 and AMA133. Each colored box represents the presence of a specific resistance gene or mutation, with functional categories indicated by color. *B*, Phenotypic resistance: Sulbactam's minimum inhibitory concentration (MIC) in the presence and absence of ceftazidime/avibactam (16/4 mg/L) or avibactam (4 mg/L).

(bla_{ADC}). The presence of multiple efflux pump genes, including components of the AdeABC and AdeIJK systems, was also observed. These combined resistance mechanisms underline the reduced susceptibility of these strains to β-lactam agents, including SUL and CAZ/AVI.

Phenotypic testing showed that all three strains were resistant to AMP/SUL and CAZ/AVI as per CLSI breakpoints (CAZ: MIC ≤8 μg/mL- susceptible and MIC ≥32 μg/mL-resistant, AMP/SUL: MIC ≤8/4 μg/mL- susceptible and MIC ≥32/16 μg/mL-resistant) [33]. The MIC values for CAZ/AVI were 32/8 μg/mL for AMA133 and >256/64 μg/mL for AMA205 and AMA3. The MIC values for AMP/SUL were 32/16, 128/64, and >256/128 μg/mL for AMA133, AMA3, and AMA205, respectively. The addition of CAZ/AVI restored susceptibility to SUL, with similar fold reductions in MIC observed across the tested CAZ/AVI concentrations. MICs for other tested agents are provided in Supplementary Table 1.

In the AMA133 strain, the presence of OXA-23-like β-lactamases, which are not effectively inhibited by AVI, was confirmed, along with the efflux transporter AbuO responsible for the active efflux of multiple antibiotics [3]. The MIC of SUL decreased from 16 μg/mL to < 0.5 μg/mL (>32-fold reduction) when combined with CAZ/AVI, and to 2 μg/mL (8-fold reduction) with AVI alone, effectively restoring SUL susceptibility.

In AMA3, the bla_{NDM-1} gene, encoding a MBL that confers resistance to nearly all β-lactams, not inhibited by AVI and bla_{PER-7}, an extended-spectrum β-lactamase with limited susceptibility to AVI was identified [34]. This strain also harbored OprD porin mutations. SUL MIC decreased from 64 μg/mL to 4 μg/mL (16-fold reduction) with both CAZ/AVI and AVI.

In AMA205, bla_{NDM-1}, as well as bla_{OXA-23} and bla_{OXA-65}, were identified. Additionally, the presence of bla_{CMY-6} and bla_{TEM-1B}, which confer resistance to cephalosporins, was detected; however, these enzymes are typically inhibited by AVI [35]. *LpxA* gene mutation that increases the membrane permeability to non-polymyxin antibiotics such as β-lactams was also present [36]. SUL MIC decreased from >128 μg/mL to 4 μg/mL (>32-fold reduction) with both CAZ/AVI and AVI.

The fold reductions in SUL's MIC indicate that CAZ/AVI provides no significant benefit compared to AVI alone in the presence of MBLs. Further, higher fold reductions in the AMA205 strain compared to AMA3 were evident.

Static Concentration Time-Kill Assays

Figure 2 shows percentage reductions in AUC_CFU for sulbactam and CAZ/AVI, both as monotherapy and in combination. Supplementary Figure 1 illustrates the change in bacterial burden over time. The combination of sulbactam and CAZ/AVI consistently outperformed either drug alone across all three CRAB strains, aligning with the lower MICs of sulbactam when combined with CAZ/AVI.

In AMA133, higher concentrations of AMP/SUL and CAZ/AVI alone reduced AUC_CFU by approximately 90% and 70%, respectively, while lower concentrations resulted in modest reduction (<30% in AUC_CFU). However, against AMA3 and AMA205, monotherapy showed negligible activity with <10% reduction in AUC_CFU. Combination regimens achieved 80%–90% AUC_CFU reduction in AMA133 and 50%–70% in AMA3 and AMA205. AMA205 showed slightly greater killing (approximately 10% more than AMA3), likely due to the *lpxA* mutation. SUL was the main driver of efficacy, as low sulbactam concentrations (12.5 μg/mL) were ineffective even with high CAZ/AVI concentrations. Sulbactam activity showed minimal difference between 50 and 100 mg/mL, indicating concentration-independent activity above a threshold.

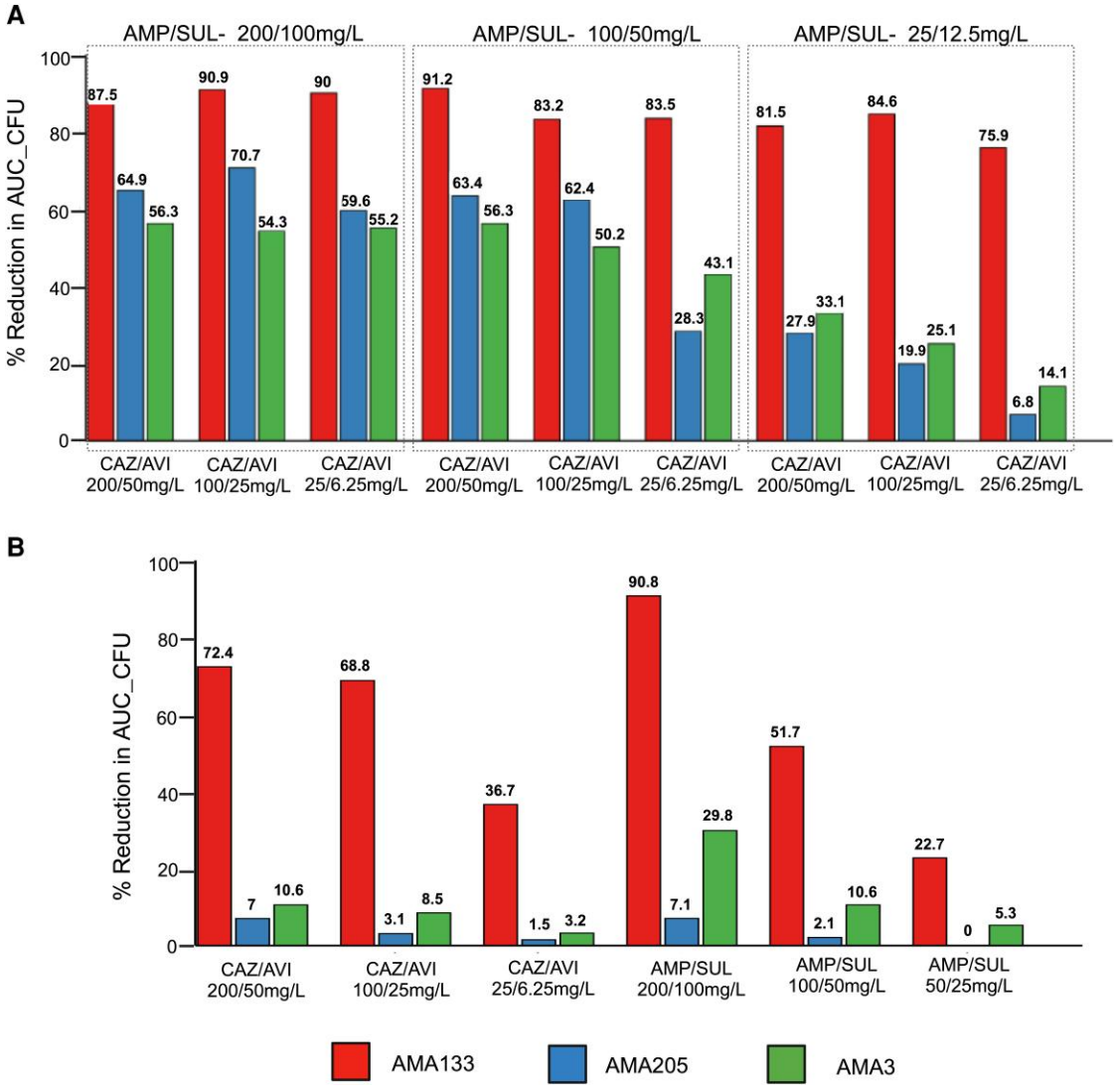

Figure 2. Pharmacodynamic activity quantified in static concentration time-kill assays shown as percentage reduction in the AUC_CFU compared to growth control for various concentrations of AMP/SUL and CAZ/AVI. *A*, in combination and *B*, as monotherapy. AUC_CFU = area under the colony-forming unit versus time curve, AMP/SUL = ampicillin/sulbactam, CAZ/AVI = ceftazidime/Avibactam.

Mechanism-based Model

Figure 3 presents the PK/PD model schematic detailing the pharmacological interactions of AMP/SUL and CAZ/AVI with molecular targets and resistance mechanisms across the three CRAB strains. The model incorporates bacterial subpopulations with varying susceptibilities to these antibiotics for each strain. For AMA3 and AMA205, two subpopulations were identified: one resistant to CAZ but susceptible to SUL, and another resistant to both drugs. In contrast, AMA133 exhibited three subpopulations, including one with intermediate susceptibility to CAZ and susceptibility to SUL.

SUL's killing was modeled using the non-hydrolyzed fraction, with *Emax* fixed based on the acylation rate constants for PBPs 1, 2, and 3. The low acylation factors for these targets indicate SUL's limited PBP-inactivation potential. However, an augmentation factor, modeled as a two-fold increase in *Emax*, was estimated, likely due to activity on additional targets and enhanced permeation. The *EC*50 values for SUL's susceptible and resistant subpopulations were lowest for AMA133, 3–4 times higher in AMA205 compared to AMA133, and highest for AMA3 (approximately 3 times higher than AMA205). These differences highlight that, in the absence of AVI, SUL's efficacy was best against the non-MBL strain AMA133.

AVI significantly enhanced SUL potency by reducing SUL's *EC*50 by approximately 100-fold in AMA205, 30-fold in AMA3, and 8-fold in AMA133. The prominent enhancer effect in strains with NDM-1 highlights AVI's critical role in targeting resistance mediated by MBLs. Furthermore, the overall

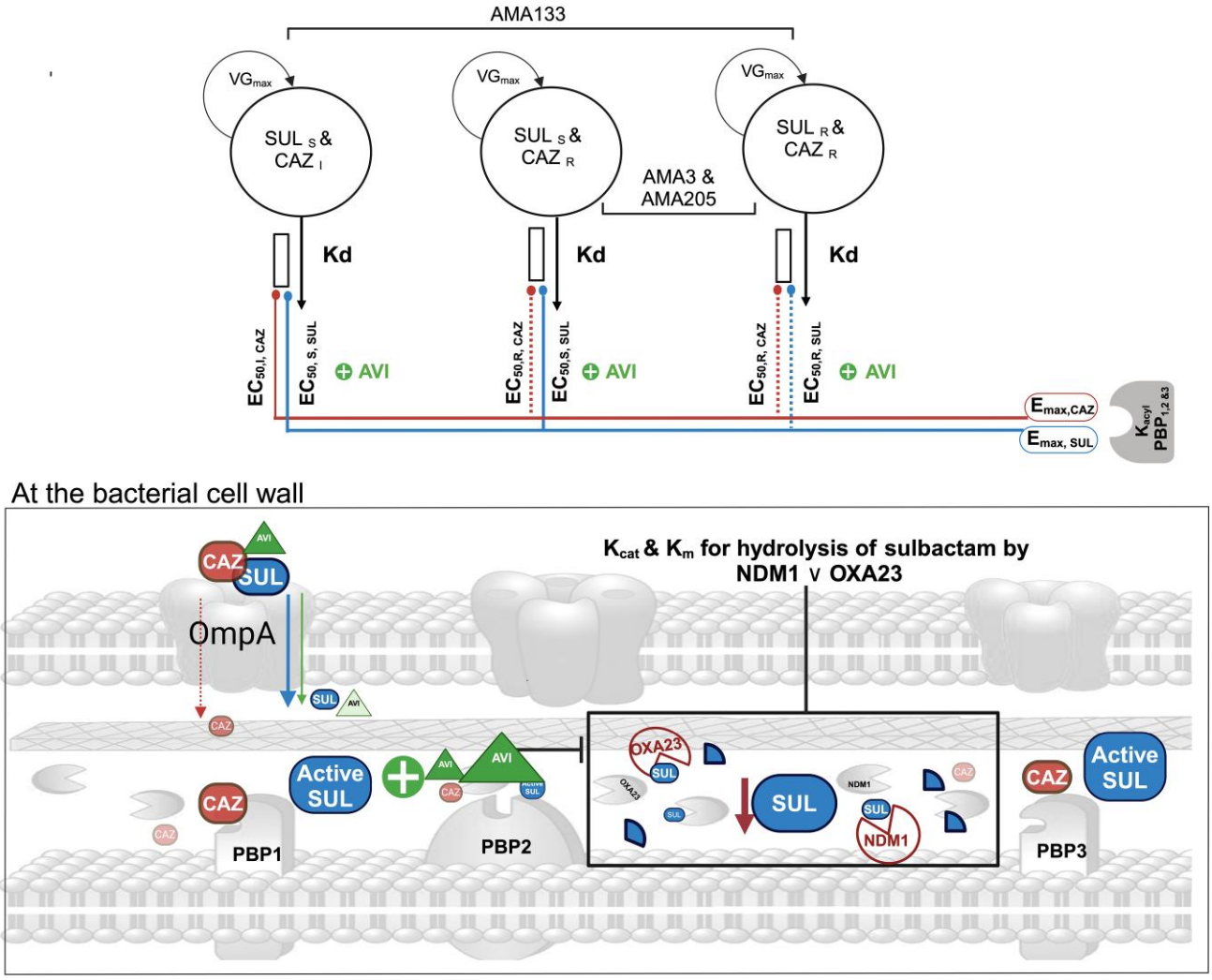

Figure 3. The model schematic illustrates the bacterial replication and death dynamics with either AMP/SUL and CAZ/AVI alone or in combination. A mixture model was used to represent three bacterial subpopulations (SUL_S/CAZ_I, SUL_S/CAZ_R, SUL_R/CAZ_R) for AMA133, and two subpopulations (SUL_S/CAZ_R, SUL_R/CAZ_R) for AMA205 and AMA3. SUL hydrolysis by OXA-23 and NDM-1 enzymes was modeled, with non-hydrolyzed SUL (blue), CAZ (red), and AVI (green) enhancing the natural death rate of bacterial subpopulations. The *Emax* values reflect drug acylation rates for PBPs, with SUL exhibiting better penetration due to its lower molecular weight. AVI enhances SUL's effect primarily through targeting PBP2. Drug abbreviations: SUL = sulbactam, CAZ = ceftazidime, AVI = avibactam.

enhancing effect of AVI was greater for AMA205 compared to AMA3, which aligns with the resistome and MIC fold reductions.

This limitation was reflected in its *EC*50 values, which were significantly higher than those of SUL. It's *EC*50 in the CAZ-resistant AMA3 subpopulation was approximately 20,000-fold higher than SUL's *EC*50 in susceptible populations. Final parameter estimates, along with their relative standard errors, are summarized in Table 2. The parameters were estimated with good precision, as demonstrated by the relative standard errors of the estimates. The model accurately predicted the time course of viable bacterial density for different mono and combination therapies against the three strains, as shown by the observed versus predicted fits in Figure 4.

Model-based Simulations and Validation of the MBM

Model-based simulations were performed using the MBM predicted parameters to guide the experimental design and optimization of AMP/SUL and CAZ/AVI dosing regimens. These simulations were validated by assessing the killing activity in response to these regimens, utilizing a one-compartment IVDIM for more reliable clinical translation.

MBM-based simulations showed minimal activity for CAZ/AVI monotherapy across all strains, resembling growth control. AMP/SUL monotherapy achieved >2- $\log_{10}$ killing against AMA133, followed by regrowth, and approximately 1- $\log_{10}$ killing against AMA205 and AMA3, followed by regrowth. However, high-dose AMP/SUL (8 g/4 g) with CAZ/AVI achieved 4–6 $\log_{10}$ reduction against AMA205 and 3–4 $\log_{10}$

Table 2. Final Parameter Estimates for the Mechanism-based Model for the Three CRAB Isolates (AMA133, AMA205, and AMA3)

Parameter (units)	Description	Estimate (%RSE) AMA133	Estimate (%RSE) AMA205	Estimate (%RSE) AMA3
$Log_{10}CFU_0$ ($Log_{10}CFU/mL$)	Initial inoculum	6.28 (3.7)	6.41 (3.6)	6.34 (3.6)
$Log_{10}CFU_{max}$ ($Log_{10}CFU/mL$)	Maximum population size	8.9 (Fix)	8.9 (Fix)	8.9 (Fix)
$Log_{10}CFU_m$ ($Log_{10}CFU/mL$)	Population size at which rate of replication is half maximal	8.05 (0.89)	7.70 (1.0)	7.75 (0.36)
$Log_{10}MF_{RR}$	Mutation frequency for SUL^R/CAZ^R	−5.88 (12)	−5.48 (7.4)	−5.39 (6.2)
$Log_{10}MF_{SR}$	Mutation frequency for SUL^S/CAZ^R	−1.33 (42)	−0.234 (54)	−0.509 (39)
$Log_{10}MF_{SI}$	Mutation frequency for SUL^S/CAZ^I	−0.432 (24)	NA	NA
Kd (h^1)	Natural death rate	0.2 (Fix)	0.2 (Fix)	0.2 (Fix)
$K_{acyl,\ CAZ}$ ($M^{-1}\cdot s^{-1}$)	Acylation rate constant for CAZ	5781 (Fix)	5781 (Fix)	5781 (Fix)
$EC50_{,\ CAZ,\ I}$ (μg/mL)	CAZ concentration resulting in 50% of E_{max}, CAZ in the intermediate susceptibility population	139 (35)	NA	NA
$EC50_{,\ CAZ,\ R}$ (μg/mL)	CAZ concentration resulting in 50% of E_{max}, CAZ in the resistant population	1380 (9.3)	7258 (14)	20 585 (18)
γ, CAZ	Hill coefficient for CAZ	3.56 (19)	1.42 (8.3)	1.05 (6.2)
$K_{acyl,\ SUL}$ ($M^{-1}\cdot s^{-1}$)	Acylation rate constant for sulbactam	26.1 (Fix)	26.1 (Fix)	26.1 (Fix)
$EC50_{,\ SUL,\ S}$ (μg/mL)	SUL concentration resulting in 50% of E_{max}, SUL in the susceptible population	0.0603 (34)	0.335 (31)	1.11 (32)
$EC50_{,\ SUL,\ R}$ (μg/mL)	SUL concentration resulting in 50% of E_{max}, SUL in the resistant population	230 (22)	1114 (18)	2220 (8.7)
AF	Augmentation factor for $K_{acyl,\ SUL}$	2 (Fix)	2.34 (7.8)	2 (Fix)
γ, SUL	Hill coefficient for SUL	0.450 (17)	0.237 (12)	0.243 (28)
Enz_{50} ($Log_{10}CFU/mL$)	Bacterial concentration resulting in 50% of Enz_{max}	4.95 (24)	6.65 (12)	7.88 (10)
Enz_{max}	Maximum enzyme production capacity by the bacterial population	3.26 (27)	2.98 (18)	4.61 (22)
AVI_{enh}	AVI's enhancer effect on SUL	0.123 (32)	0.0103 (39)	0.0336 (52)
$K_{cat,\ NDM1}$ (s^{-1})	Turnover number for SUL hydrolysis by NDM-1	NA	430 (Fix)	430 (Fix)
$K_{m,\ NDM1}$ (mM)	Michaelis–Menten constant for SUL hydrolysis by NDM-1		3 (Fix)	3 (Fix)
$K_{cat,\ OXA23}$ (s^{-1})	Turnover number for SUL hydrolysis by OXA-23	16 (Fix)	16 (Fix)	NA
$K_{m,\ OXA23}$ (mM)	Michaelis–Menten constant for SUL hydrolysis by OXA-23	1.7 (Fix)	1.7 (Fix)	NA
Σ	Log-additive error (variance)	0.400 (7.2)	0.077 (7.3)	0.111 (7.5)

The extent of precision for each parameter is represented by the relative standard error (RSE%).

Abbreviations: SUL, sulbactam, CAZ, ceftazidime, AVI, avibactam.

reduction against AMA3. Moderate-dose AMP/SUL (4 g/2 g) with CAZ/AVI resulted in 6 log_{10} killing in AMA133 and 3–4 log_{10} in AMA205, but only 2–3 log_{10} in AMA3. Even the lowest AMP/SUL dose (2 g/1 g)-based combination achieved substantial killing against AMA133, with 4–5 log_{10} reduction highlighting its increased susceptibility compared to MBL-positive strains (AMA205 and AMA3). Simulation results for the high-dose (8 g/4 g) AMP/SUL mono and combination therapies are presented in Supplementary Figure 2. The bacterial killing observed in the one-compartment IVDIM was largely consistent with MBM predictions (Figure 5), showing similar trends across all strains. However, some discrepancies were noted. The model did not capture the delay in killing at lower doses and incorporating a 4-hour lag-time improved early-phase

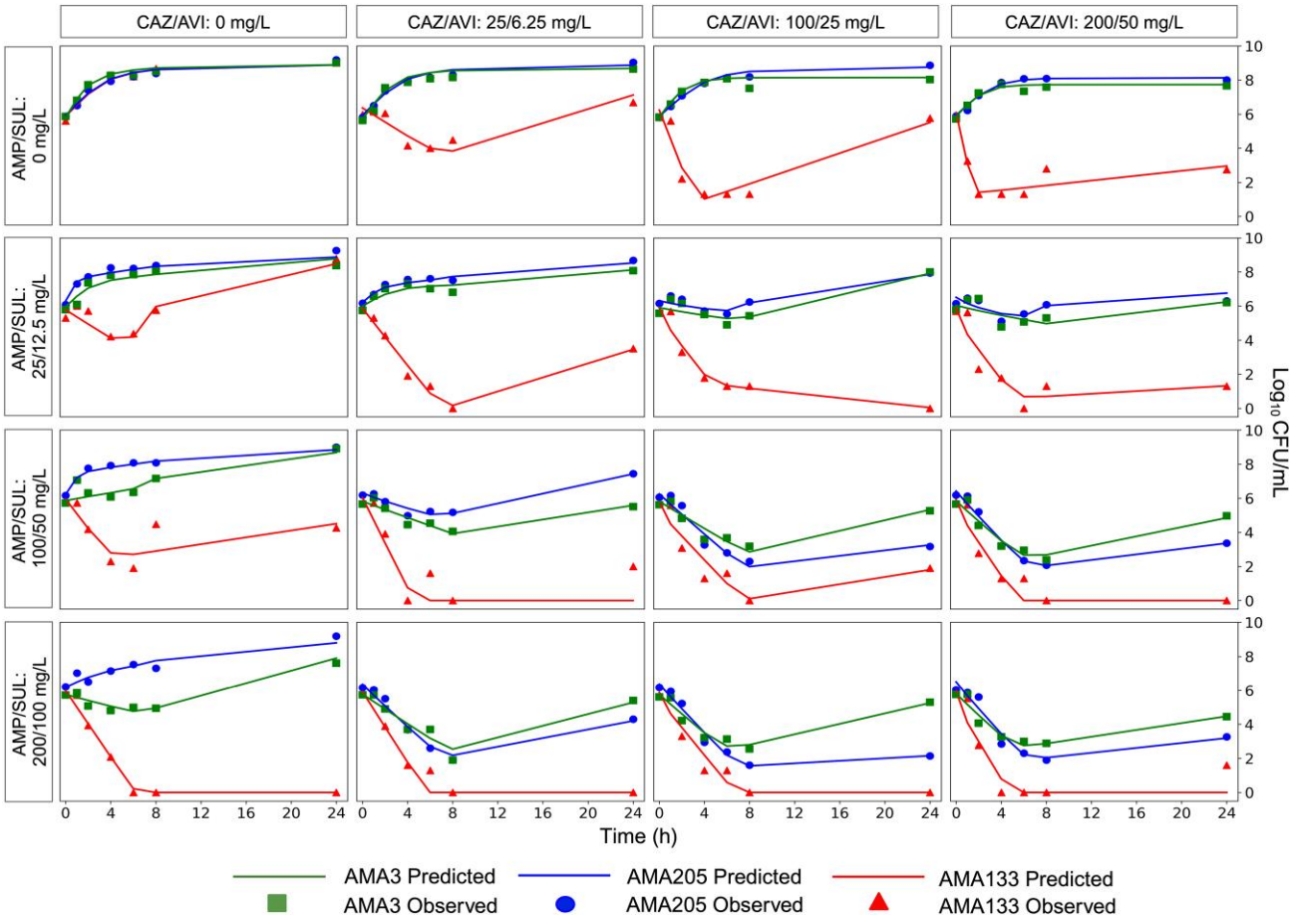

Figure 4. Observed versus model predicted curves for change in bacterial burden overtime based on static concentration time-kill assays with CAZ/AVI alone (top row), AMP/SUL alone (first column), and their combination against AMA3 (green), AMA205 (blue) and AMA133 (red). Symbols are total bacteria (Log_{10} CFU/mL) quantified, and the solid lines are the mechanism-based model predicted fits. AMP/SUL = ampicillin/sulbactam, CAZ/AVI = ceftazidime/avibactam.

predictions (Supplementary Figure 3). Despite these limitations, these results highlight the MBM's potential to guide experimental design and optimize dosing regimens, taking patient characteristics and bacterial resistance mechanisms into consideration.

DISCUSSION

This study demonstrates the therapeutic potential of combining AMP/SUL with CAZ/AVI against CRAB strains harboring MBLs and class-D carbapenemases, which represent some of the most formidable resistance mechanisms in Gram-negative bacteria. Historically, the colistin-meropenem combination was considered the cornerstone of treatment for *A. baumannii* infections. However, randomized controlled trials have reported poor outcomes with clinical failure rates of 83% for colistin monotherapy and 81% for the colistin–meropenem combination, and corresponding 28-day mortality rates of 46% and 52% [13].

A. baumannii's ability to survive without lipooligosaccharides (LOS)/lipopolysaccharides (LPS) renders its outer membrane a poor therapeutic target [37]. In contrast, peptidoglycan synthesis remains essential for maintaining cell structure and integrity, making β-lactam antibiotics a viable treatment option. These agents exert bactericidal effects by acylating the active serine sites of PBPs, forming covalent bonds, thereby disrupting cell wall synthesis. This time-dependent acylation process is fundamental to the pharmacodynamic activity of β-lactams and is quantitatively captured by the MBM. Prolonged or irreversible PBP acylation can elicit a significant post-antibiotic effect [38]. Importantly, the favorable safety profile of β-lactams allows for dose escalation without toxicity concerns.

AMP/SUL has demonstrated potent in vitro activity against CRAB, showing a low frequency of spontaneous resistance in a hollow-fiber infection model [39]. A systematic review further supports the superior efficacy of high-dose SUL-based regimens compared to colistin-based regimens [13]. Additionally, sulbactam may benefit from enhanced permeation through OmpA, a non-specific slow porin, due to its low molecular weight, offering an advantage over other β-lactams [40].

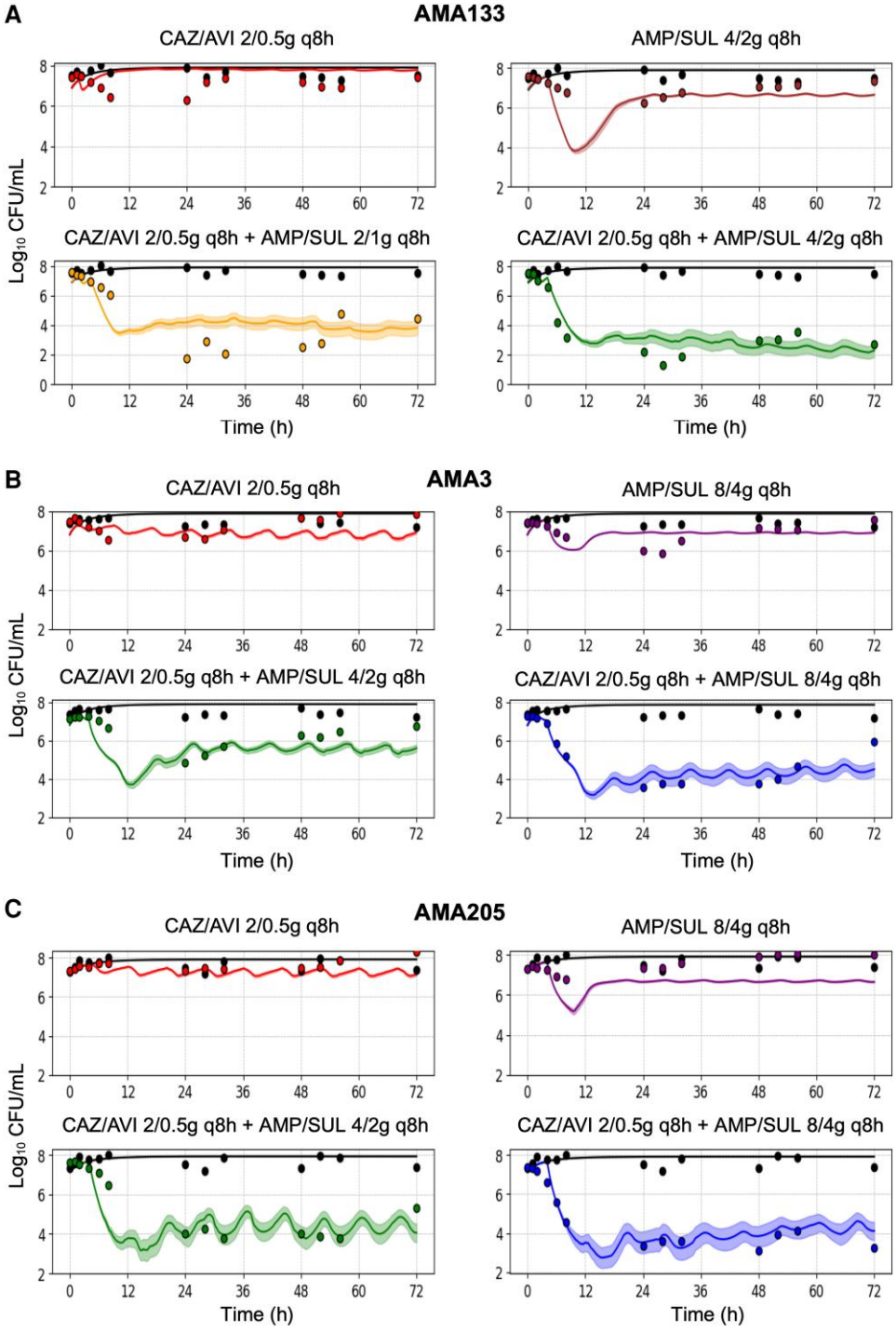

Figure 5. In silico simulations performed using the mechanism-based model developed based on the time course of bacterial killing activity quantified by performing static concentration time-kill assays. The mean predicted viable bacterial count profiles in response to clinically relevant exposure simulated for AMP/SUL and CAZ/AVI as mono and combination therapies are shown for (*A*) AMA133, (*B*) AMA3, and (*C*) AMA205. The shaded region indicates the 95% CI, and points represent observed experimental values based on quantification of viable bacteria following exposure to these regimens in a one-compartment in vitro dynamic infection model (IVDIM). AMP/SUL = ampicillin/sulbactam, CAZ/AVI = ceftazidime/avibactam.

Despite these advantages, treating NDM-1-producing strains remains a significant challenge. In a prior study involving 40 NDM-producing *A. baumannii* isolates, sulbactam alone exhibited a MIC50 of 256 μg/mL, which was reduced to 32 μg/mL when combined with avibactam. This study tested MDR *Acinetobacter spp* clinical isolates with diverse resistance genes

[17]. These findings informed the clinical use of CAZ/AVI + AMP/SUL in a pediatric CRAB case, where previous treatments, including tigecycline, meropenem, trimethoprim/sulfamethoxazole, aztreonam, and colistin, had failed. This combination led to marked clinical improvement within 48 hours and eventual resolution of the infection [41].

Two strains used in our study were resistant to cefiderocol [Supplementary Table 1], and a recent clinical outbreak highlighted high microbiological failure rates with cefiderocol treatment. In that same outbreak, AMP/SUL + CAZ/AVI, selected based on in vitro synergy testing, achieved clinical cure in cases of bacteremia and ventilator-associated pneumonia [42]. These findings highlight the translational potential of this combination, even in scenarios where newer agents like cefiderocol have limited efficacy.

Our findings demonstrate the efficacy of AMP/SUL and CAZ/AVI combinations in both static and dynamic in vitro infection models. High-dose AMP/SUL (8 g/4 g) combinations were especially effective against MBL-producing pathogens. Although AVI does not directly inhibit NDM-1, its role as a β-lactam enhancer may significantly boost the activity of both SUL and CAZ.

SUL and CAZ primarily target PBP1 and PBP3, which are essential for septal and lateral peptidoglycan synthesis, respectively. AVI inhibits PBP2, disrupting cell elongation and re-sensitizing bacteria to divisome-targeting antibiotics. This PBP2-mediated synergy has been demonstrated in NDM-1-producing *K. pneumoniae*, where AVI combined with LL-37, an antimicrobial peptide, achieved complete killing in SCTK assays [43]. Similarly, the inclusion of mecillinam (a PBP-2 targeting agent) with aztreonam against NDM-producing *K. pneumoniae* in a hollow-fiber infection model resulted in enhanced bactericidal activity and a pronounced post-antibiotic effect, emphasizing the therapeutic potential of PBP2 inhibition in regimens targeting NDM-1-producing pathogens [44]. In *A. baumannii*, disruption of the elongasome sensitizes bacteria to antibiotics targeting divisome peptidoglycan synthesis. Checkerboard assays confirmed synergistic interactions between elongasome-targeting agents with divisome blockers, such as SUL [45]. Additionally, mutations in *lpxA* compromise the outer membrane's permeability barrier, thereby enhancing β-lactam penetration and activity. While *lpxA* mutants are resistant to colistin, they exhibit improved susceptibility to β-lactams [36]. Furthermore, LOS deficiency has been linked to hypersensitivity to elongasome inhibitors, as elongasome synthesis becomes critical for maintaining cell rigidity in the absence of LOS [37]. The improved susceptibility of AMA205 to the AMP/SUL and CAZ/AVI combination, despite harboring both $bla_{\text{NDM-1}}$ and $bla_{\text{OXA-23}}$, could be attributed to the presence of the *lpxA* mutation.

Rapid diagnostics, such as immunochromatographic assays, now allow for β-lactamase identification within minutes. For example, the Resist Acineto test is an effective tool for the rapid detection of CRAB species and their associated resistance mechanisms [46]. When paired with mechanism-based modeling, these diagnostics can support tailoring antibiotic therapy by using resistance profiles. MBMs extend beyond describing bacterial dynamics observed in vitro or in vivo, they are designed to translate experimental findings into clinically meaningful outcomes. By simulating multiple treatment scenarios, MBMs facilitate the selection of optimal regimens that would otherwise be challenging to evaluate experimentally. This approach has proven effective in carbapenem-resistant *K. pneumoniae* isolates, where an MBM developed based on SCTK data accurately predicted the bacterial killing and regrowth in the dynamic IVDIM system, validating the developed MBM [47].

Although this study focused on three CRAB strains from the globally prevalent and high-risk lineages (ST25 and ST79) [48, 49], CRAB possesses a highly plastic genome, with substantial genotypic and phenotypic variability even within monophyletic lineages [50]. Future studies should include diverse CRAB isolates to strengthen the generalizability and clinical relevance of our findings. The mechanism underlying the CAZ/AVI-SUL interaction remains incompletely understood. While PBP2 engagement by AVI has been proposed, potential contributors include altered membrane permeability, efflux modulation, inhibition of non-MBL β-lactamases, and indirect stabilization of partner β-lactams. These remain hypothetical and require targeted experimental validation. Integrating WGS with detailed phenotypic profiling across larger clinical and knockout CRAB stains, coupled with computational approaches, will facilitate the identification of key drivers of synergistic interactions and therapeutic success. Incorporating bacterial-metabolomics will provide deeper insights into these molecular mechanisms and pathogen adaptation under antibiotic pressure [23]. Further refinement of the model could incorporate the inoculum effect, which influences antibiotic activity and varies across different in vitro systems. While IVDIMs used in this study simulated drug exposures relevant to critically ill patients, they do not fully capture the complexity of in vivo immunodynamics. Additional limitations include the absence of drug concentration measurements in the one-compartment IVDIM setup and the reliance on literature-derived β-lactamase hydrolysis rates from recombinant OXA-23 and NDM-1 enzymes, rather than direct quantification from the study strains.

The combination of CAZ/AVI and high-dose AMP/SUL against challenging CRAB isolates holds strong translational potential, as both agents are widely available and have well-established safety profiles in clinical practice. The MBM facilitates this translation by integrating patient-specific factors and the pathogen genetic profiles into clinical decision-support algorithms. This approach enables the development of individualized antibiotic regimens aimed at optimizing therapeutic outcomes.

Supplementary Data

Supplementary materials are available at *The Journal of Infectious Diseases* online (http://jid.oxfordjournals.org/). Supplementary materials consist of data provided by the author that are published to benefit the reader. The posted materials are not copyedited. The contents of all supplementary data are the sole responsibility of the authors. Questions or messages regarding errors should be addressed to the author.

Notes

Author Contributions. G. G. R. conceived the study, and G. G. R. and B. A. designed the experiments. B. A., E. L., Q. V., R. S., and N. M. B. performed the experiments. B.A., Q.V., S.M.R., V.M., I.L., G.M.T, and G.G.R. analyzed the data and interpreted the results. G.G.R., M.S.R., and F.P. contributed to materials/sequencing tools. B.A. and G.G.R. wrote and revised the manuscript. M.S.R., R.A.B., D.P., and F.P. provided edits. All authors read and approved the final manuscript.

Financial support. The authors' work was supported by National Institutes of Health R01AI146241 and R01AI170889 to Gauri G. Rao and SC3GM125556 to María Soledad Ramirez.

Potential conflicts of interest. The authors declare no conflict of interest. All authors: No reported conflicts. All authors have submitted the ICMJE Form for Disclosure of Potential Conflicts of Interest. Conflicts that the editors consider relevant to the content of the manuscript have been disclosed. The content is solely the authors' responsibility and does not necessarily represent the official views of the National Institutes of Health.

References

1. Wong D, Nielsen TB, Bonomo RA, Pantapalangkoor P, Luna B, Spellberg B. Clinical and pathophysiological overview of *Acinetobacter* infections: a century of challenges. Clin Microbiol Rev **2016**; 30:409–47.
2. CDC. Carbapenem-resistant *Acinetobacter*: an urgent public health threat. Available at: https://arpsp.cdc.gov/story/cra-urgent-public-health-threat. Accessed 16 February 2025.
3. Kyriakidis I, Vasileiou E, Pana ZD, Tragiannidis A. *Acinetobacter baumannii* antibiotic resistance mechanisms. Pathogens **2021**; 10:373.
4. Ramirez MS, Bonomo RA, Tolmasky ME. Carbapenemases: transforming *Acinetobacter baumannii* into a yet more dangerous menace. Biomolecules **2020**; 10:720.
5. Wang Y, Wang J, Wang R, Cai Y. Resistance to ceftazidime-avibactam and underlying mechanisms. J Glob Antimicrob Resist **2019**; 22:18–27.
6. Sader HS, Castanheira M, Flamm RK, Mendes RE, Farrell DJ, Jones RN. Ceftazidime/avibactam tested against Gram-negative bacteria from ICU and non-ICU patients, including those with ventilator-associated pneumonia. Int J Antimicrob Agents **2015**; 46:53–9.
7. Kwon HI, Kim S, Oh MH, et al. Outer membrane protein A contributes to antimicrobial resistance of *Acinetobacter baumannii* through the OmpA-like domain. J Antimicrob Chemother **2017**; 72:3012–5.
8. Infectious Diseases Society of America. Managing carbapenem-resistant gram-negative infections: Challenges in the developing world. 2023. Available at: https://www.idsociety.org/science-speaks-blog/2023/managing-carbapenem-resistant-gram-negative-infections-challenges-in-the-developing-world/. Accessed 29 July 2025.
9. Dumbleton JT, Shah AP, Ho BM, Singh N, de Souza H, Smith NM. Pharmacodynamics of aztreonam/ceftazidime/avibactam and polymyxin B versus New Delhi MBL-producing *Acinetobacter baumannii*. JAC Antimicrob Resist **2025**; 7:dlaf068.
10. Bassetti M, Echols R, Matsunaga Y, et al. Efficacy and safety of cefiderocol or best available therapy for the treatment of serious infections caused by carbapenem-resistant Gram-negative bacteria (CREDIBLE-CR): a randomised, open-label, multicentre, pathogen-focused, descriptive, phase 3 trial. Lancet Infect Dis **2021**; 21:226–40.
11. Shields RK, Dorazio AJ, Tiseo G, et al. Frequency of cefiderocol heteroresistance among patients treated with cefiderocol for carbapenem-resistant *Acinetobacter baumannii* infections. JAC Antimicrob Resist **2024**; 6:dlae146.
12. Grabein B, Arhin FF, Daikos GL, Moore LSP, Balaji V, Baillon-Plot N. Navigating the current treatment landscape of metallo-β-lactamase-producing Gram-negative infections: what are the limitations? Infect Dis Ther **2024**; 13:2423–47.
13. Hobson CA, Cointe A, Jacquier H, et al. Cross-resistance to cefiderocol and ceftazidime–avibactam in KPC β-lactamase mutants and the inoculum effect. Clin Microbiol Infect **2021**; 27:1172.e7–e10.
14. Shields RK, Paterson DL, Tamma PD. Navigating available treatment options for carbapenem-resistant *Acinetobacter baumannii-calcoaceticus* complex infections. Clin Infect Dis **2023**; 76:S179–93.
15. Warrier AR, Sneha R, Wilson A, Prakash S. Clinical efficacy and safety of high-dose ampicillin-sulbactam among patients with CRAB infections: a case series. Open Forum Infect Dis **2022**; 9:(Suppl 2):654.
16. Moussa SH, Shapiro AB, McLeod SM, et al. Molecular drivers of resistance to sulbactam-durlobactam in contemporary clinical isolates of *Acinetobacter baumannii*. Antimicrob Agents Chemother **2023**; 67:e0066523.
17. Pasteran F, Cedano J, Baez M, et al. A new twist: the combination of sulbactam/avibactam enhances sulbactam activity against carbapenem-resistant *Acinetobacter baumannii* isolates. Antibiotics **2021**; 10:577.
18. Patel JB; Clinical and Laboratory Standards Institute. Performance standards for antimicrobial susceptibility

testing. Wayne, PA: Clinical and Laboratory Standards Institute, **2017**.
19. Sy SKB, Zhuang L, Sy S, Derendorf H. Clinical pharmacokinetics and pharmacodynamics of ceftazidime-avibactam combination: a model-informed strategy for its clinical development. Clin Pharmacokinet **2019**; 58:545–64.
20. Falcone M, Paterson D. Spotlight on ceftazidime/avibactam: a new option for MDR Gram-negative infections. J Antimicrob Chemother **2016**; 71:2713–22.
21. Setiawan E, Cotta MO, Abdul-Aziz M-H, et al. Population pharmacokinetics and dosing simulations of ampicillin and sulbactam in hospitalised adult patients. Clin Pharmacokinet **2023**; 62:573–86.
22. Onita T, Ikawa K, Ishihara N, et al. Pulmonary pharmacokinetic and pharmacodynamic evaluation of ampicillin/sulbactam regimens for pneumonia caused by various bacteria, including Acinetobacter baumannii. Antibiotics **2023**; 12:303.
23. Hanafin PO, Abdul Rahim N, Sharma R, et al. Proof-of-concept for incorporating mechanistic insights from multi-omics analyses of polymyxin B in combination with chloramphenicol against Klebsiella pneumoniae. CPT Pharmacometrics Syst Pharmacol **2023**; 12:387–400.
24. Covvey JR, Guarascio AJ. Sulbactam-durlobactam for the treatment of Acinetobacter baumannii-calcoaceticus complex. Expert Rev Anti Infect Ther **2024**; 22:925–34.
25. US Food and Drug Administration. Ampicillin/sulbactam label. Available at: https://www.accessdata.fda.gov/drugsatfda_docs/label/2020/050608s047lbl.pdf. Accessed 18 March 2016.
26. Infectious Diseases Society of America (IDSA). Antimicrobial resistance guidance. Available at: https://www.idsociety.org/practice-guideline/amr-guidance/. Accessed 18 March 2025.
27. Betrosian AP, Frantzeskaki F, Xanthaki A, Georgiadis G. High-dose ampicillin-sulbactam as an alternative treatment of late-onset VAP from multidrug-resistant *Acinetobacter baumannii*. Scand J Infect Dis **2007**; 39:38–43.
28. Penwell WF, Shapiro AB, Giacobbe RA, et al. Molecular mechanisms of sulbactam antibacterial activity and resistance determinants in *Acinetobacter baumannii*. Antimicrob Agents Chemother **2015**; 59:1680–9.
29. Shapiro AB. Kinetics of sulbactam hydrolysis by β-lactamases, and kinetics of β-lactamase inhibition by sulbactam. Antimicrob Agents Chemother **2017**; 61: e01234-17.
30. Bulitta JB, Landersdorfer CB. Performance and robustness of the Monte Carlo importance sampling algorithm using parallelized S-ADAPT for basic and complex mechanistic models. AAPS J **2011**; 13:212–26.
31. Traglia GM, Pasteran F, Moheb S, et al. Insights into *Acinetobacter baumannii* AMA205's unprecedented antibiotic resistance. Int J Mol Sci **2024**; 25:11424.
32. Rodgers D, Pasteran F, Calderon M, et al. Characterisation of ST25 NDM-1-producing *Acinetobacter* spp. strains leading the increase in NDM-1 emergence in Argentina. J Glob Antimicrob Resist **2020**; 23:108–10.
33. Clinical and Laboratory Standards Institute (CLSI). M100: antimicrobial susceptibility testing standards. Wayne, PA: CLSI, **2019**.
34. Valzano F, La Bella G, Lopizzo T, et al. Resistance to ceftazidime–avibactam and other new β-lactams in *Pseudomonas aeruginosa* clinical isolates: a multi-center surveillance study. Microbiol Spectr **2024**; 12:e02466-23.
35. Zasowski EJ, Rybak JM, Rybak MJ. The β-lactams strike back: ceftazidime-avibactam. Pharmacotherapy **2015**; 35: 755–70.
36. Moffatt JH, Harper M, Harrison P, et al. Colistin resistance in *Acinetobacter baumannii* is mediated by complete loss of lipopolysaccharide production. Antimicrob Agents Chemother **2010**; 54:4971–7.
37. Simpson BW, Nieckarz M, Pinedo V, McLean AB, Cava F, Trent MS. *Acinetobacter baumannii* can survive with an outer membrane lacking lipooligosaccharide due to structural support from elongasome peptidoglycan synthesis. mBio **2021**; 12:e02982-21.
38. Tilanus A, Drusano G. Optimizing the use of beta-lactam antibiotics in clinical practice: a test of time. Open Forum Infect Dis **2023**; 10:ofad340.
39. Lenhard JR, Smith NM, Bulman ZP, et al. High-dose ampicillin-sulbactam combinations combat polymyxin-resistant Acinetobacter baumannii in a hollow-fiber infection model. Antimicrob Agents Chemother **2017**; 61: e01268-16.
40. Sugawara E, Nikaido H. Ompa is the principal nonspecific slow porin of Acinetobacter baumannii. J Bacteriol **2012**; 194:4089–96.
41. Ghunaim AH. Successful treatment of Acinetobacter baumannii infection in a burn child with avibactam/sulbactam: a case report. Int Med Case Rep J **2022**; 7:347–50.
42. Dudoignon E, Caméléna F, Lafaurie M, et al. Evolution, control, and success of combination therapy with ampicillin-sulbactam/ceftazidime-avibactam during a carbapenem-resistant Acinetobacter baumannii outbreak in a burn ICU. Eur J Clin Microbiol Infect Dis **2024**; 43: 1453–9.
43. Ulloa ER, Dillon N, Tsunemoto H, Pogliano J, Sakoulas G, Nizet V. Avibactam sensitizes carbapenem-resistant NDM-1–producing Klebsiella pneumoniae to innate immune clearance. J Infect Dis **2019**; 220:484–93.
44. Klem JF, Candidate PD, Kaur JN, et al. Targeting penicillin-binding protein 2 (PBP2) to treat metallo-β-lactamase–producing Klebsiella pneumoniae: mecillinam as an American Ninja Warrior [abstract 2547]. Open Forum Infect Dis **2023**; 10:S179–S193.

45. Geisinger E, Mortman NJ, Dai Y, et al. Antibiotic susceptibility signatures identify potential antimicrobial targets in the Acinetobacter baumannii cell envelope. Nat Commun **2020**; 11:3820.
46. Bouvier M, Kerbol A, Findlay J, Freire S, Poirel L, Nordmann P. Resist Acineto rapid immunological test for the detection of acquired carbapenemase producers among Acinetobacter spp. Diagn Microbiol Infect Dis **2023**; 107:116043.
47. Garcia E, Diep JK, Sharma R, Rao GG. Model-based learn and confirm: designing effective treatment regimens against multidrug resistant Gram-negative pathogens. Int J Antimicrob Agents **2024**; 63:107100–.
48. Landelle C, Legrand P, Lesprit P, et al. Protracted outbreak of multidrug-resistant *Acinetobacter baumannii* after intercontinental transfer of colonized patients. Infect Control Hosp Epidemiol **2013**; 34:119–24.
49. Lupo A, Valot B, Saras E, et al. Multiple host colonization and differential expansion of multidrug-resistant ST25 *Acinetobacter baumannii* clades. Sci Rep **2023**; 13:491.
50. Sahl JW, Del Franco M, Pournaras S, et al. Phylogenetic and genomic diversity in isolates from the globally distributed Acinetobacter baumannii ST25 lineage. Sci Rep **2015**; 5:15188.